Comparison of the effects of downstream H_2- and O_2-based plasmas on the removal of photoresist, silicon, and silicon nitride

Bayu Thedjoisworo[a] and David Cheung
Lam Research, Surface Integrity Group (SIG), 4000 North 1st St., San Jose, California 95134

Vince Crist
Nanolab Technologies, Surface Science, 1708 McCarthy Blvd., Milpitas, California 95035

(Received 1 September 2012; accepted 29 January 2013; published 14 February 2013)

For the 45 nm technology node and beyond, there is a need to strip photoresist quickly while suppressing the loss of materials such as polycrystalline silicon (poly-Si) and silicon nitride (Si_3N_4). To achieve this goal, the authors characterized and compared the effects of downstream pure-H_2, H_2/N_2, and O_2/N_2 plasmas on the etch behaviors of photoresist, poly-Si, and Si_3N_4. The addition of N_2 to H_2 plasma increases the photoresist ash rate to a maximum that is reached at ~30–40% N_2, and the ash rate drops with further addition of N_2. At 30% N_2 addition, the ash rate increases by a factor of ~3 when compared to that obtained with pure-H_2 plasma. For O_2/N_2 plasma, the photoresist ash rate also exhibits a maximum, which is attained with 5% N_2 addition, and the ash rate drops drastically as more N_2 is added. A small addition of N_2 increases the H and O radical densities in the H_2- and O_2-based plasmas, respectively, resulting in the higher ash rates. The ash rate achieved by the O_2/N_2 chemistry is generally higher than that attained with the H_2/N_2 chemistry, and the difference becomes more significant at high temperatures. The activation energy for photoresist strip under O_2/N_2 plasma was measured to be ~10 kcal/mol, which is higher when compared to the ~5 kcal/mol measured for both the H_2/N_2 (30% N_2) and the pure-H_2 chemistries. At 300 °C, when compared to the O_2-based chemistry, the H_2-based chemistry was shown to remove Si_3N_4 with a much lower rate, ~0.7 Å/min, highlighting the benefit of the latter in conserving material loss. The ability of the H_2-based chemistry to suppress material loss and its nonoxidizing property could justify the trade off for its lower ash rates when compared to those obtained using the O_2-based chemistry. For the H_2-based chemistry, a small N_2 addition to the H_2 plasma was found to not only increase the ash rate but also suppress the Si etch rate by a factor of 8 to 22, depending on the temperature. Collectively, the H_2/N_2 chemistry shows a great promise for photoresist-strip applications in the advanced nodes, and it should be run at high temperatures (e.g., $T \geq 300$ °C) to maximize the ash rate while still maintaining extremely low Si and Si_3N_4 losses. © *2013 American Vacuum Society*. [http://dx.doi.org/10.1116/1.4792254]

I. INTRODUCTION

Because of their tremendous advantages, new classes of materials for ultra-low-*k* interlayer dielectrics[1] and high-*k*/metal gate (HKMG) stacks[2–4] have been introduced into the advanced technology nodes, and integration of these materials into the current semiconductor fabrication schemes is a formidable challenge. It was found that the oxygen-based plasma processing conventionally used for the removal of photoresist masks is incompatible with the above materials. For example, O_2-based plasmas cause undesirable chemical modifications of ultra-low *k* (ULK) materials.[5–9] In addition, oxygen-based plasma ashing causes the oxidation of semiconductor substrates and metals, attributes that are unacceptable for advanced-device fabrication.[4,10,11] On the other hand, H_2-based plasma processing has garnered much attention because it is chemically more benign toward the above materials and, hence, it is potentially more suitable for use in advanced-device fabrication. For example, downstream H_2-based plasma processing has been shown to yield acceptable ash rates while minimizing deleterious impacts on ULK films[5,6,12,13] and oxidation of metal structures.[10,11]

Aside from maintaining compatibility with the HKMG materials, a major challenge in the front-end-of-the-line (FEOL) fabrication of advanced devices is to strip the implanted photoresist reasonably quickly while maintaining extremely low loss of materials (e.g., the Si substrate and Si_3N_4 sidewall spacer) and dopants.[14–16] Such a challenge is encountered in applications that include the lightly doped drain (LDD) implant photoresist-strip and high-dose ion implantation strip (HDIS). For example, for the 32 nm LDD implant strip applications, there is a very stringent requirement for Si loss to be <1 Å per implant-mask-strip step and the loss of the Si_3N_4 spacer to be negligible.

The goal of this work is to evaluate the feasibility of the hydrogen process for the above photoresist-strip applications. To achieve this goal, it is important that we elucidate the etch behaviors of the photoresist, Si, and Si_3N_4 in H_2-based plasmas, and compare the behaviors with those obtained when using the more conventional O_2-based plasma. Prompted by the tremendous promise held by the H-based plasma, we previously worked to gain an initial understanding of the H_2 process. In that work, we elucidated the interactions between

[a]Electronic mail: Bayu.thedjoisworo@lamresearch.com

downstream *pure-H_2* plasma with photoresist, Si, and Si_3N_4 surfaces,[17] and this paper essentially serves as a follow-up. A drawback of the pure-H_2 plasma processing is that its ash rate is relatively low, ~3000 Å/min, even at a high temperature of >300 °C. It was reported that the addition of N_2 to the H_2 plasma alters the removal rates of organic materials exposed to the plasma[18,19] and, therefore, this work investigates the effect of N_2 addition to the H_2 plasma on the etch behaviors of photoresist, Si, and Si_3N_4. Since O_2-based plasma is the conventional method for ashing photoresists, we also compare the etch behaviors of the above substrates under H_2/N_2 and O_2/N_2 plasmas to determine which chemistry is more viable for photoresist-strip applications in the advanced technology nodes.

Here, we employ remote/downstream plasma processing in which the wafer is positioned downstream of the plasma. When compared with direct plasma processing, downstream plasma generally results in lower material losses.[20] In addition, downstream conditions alleviate the detrimental effects of direct plasma exposure (e.g., charging damage, ion-impact damage, and defects introduced by high fluxes of energetic photons)[21–24] and the insignificant ion bombardment minimizes damage to ULK materials.[5,6,25,26] These attributes make downstream plasma processing especially attractive for silicon integrated circuits at 45 nm and beyond.

This work characterizes and compares the etch behaviors of photoresist, Si, and Si_3N_4 in downstream O_2/N_2, H_2/N_2, and pure-H_2 plasmas. We investigated the effect of N_2 addition to either the H_2 or the O_2 plasma on the photoresist ash rate. From the data of photoresist ash rate as a function of temperature, the activation energy for the photoresist-strip reaction for each of the above three chemistries was determined. Si_3N_4 etch was performed as a function of N_2 concentration for both the H_2- and O_2-based plasma chemistries, and the etch behaviors were then compared. We also compared the poly-Si etch behavior under pure-H_2 and H_2/N_2 plasmas as a function of temperature. Based on the process trends obtained, we were ultimately able to recommend a plasma chemistry as well as the process conditions that achieve high ash rates while minimizing Si and Si_3N_4 losses.

II. EXPERIMENT

The substrates used in this work were 300 mm photoresist-coated, poly-Si, and Si_3N_4 wafers. In particular, we used the193 nm deep ultraviolet (DUV) photoresist (Tokyo Ohka Kogyo) that comprised a poly(hydroxystyrene)-based polymer as the resin. The poly-Si wafer corresponds to a bare silicon substrate that was deposited with a layer of thermal oxide (1500 Å) followed by a plasma-enhanced chemical vapor deposition (PECVD) of an undoped poly-Si layer (1500 Å). The Si_3N_4 wafer was prepared in house by depositing a Si_3N_4 film (PECVD) on a bare silicon substrate. The poly-Si wafers were HF-dipped in a 1:50 HF:H_2O mixture at room temperature for 60 s to remove the native oxide layer and were then plasma processed within 5 h to prevent any significant regrowth of native oxide.

The downstream inductively coupled plasma (ICP) reactor that was used here has been described in our previous publication.[17] Briefly, the reactor consists of three main components: plasma source, showerhead, and reaction chamber. The plasma source comprises a quartz dome surrounded by induction coils that are powered by a radio frequency power supply. The showerhead separates the plasma source from the reaction chamber, and it shields the wafer from direct plasma exposure and ion bombardments.[6,21,24,25,27,28] The wafer is placed downstream of the plasma inside the reaction chamber, and it rests on a platen (stage) which is fitted with a heating element that allows the substrate temperature to be varied. The platen temperature (T) is controlled by means of thermocouples attached to the platen and a temperature controller. Through the use of a variable gate valve, the flow rate and chamber pressure can be controlled independently.

In a typical experiment, the platen was first heated to reach the desired temperature set point. Etchant gases were then introduced into the reactor and the chamber was evacuated by means of a vacuum pump to the desired pressure. Unless otherwise stated, the chamber was stabilized at a pressure of 1.5 Torr for the experiments performed here. Specifically, the H_2/N_2 plasma was generated by flowing a mixture of H_2 and forming gases, while the O_2/N_2 plasma was generated using a mixture of O_2 and N_2 gases. The substrate wafer was placed onto the stage and heated to reach the desired temperature. The source power was then turned on to generate the plasma and initiate the etch reaction.

Thicknesses of the photoresist, poly-Si, and Si_3N_4 films were measured before and after plasma exposure by means of ellipsometry (Therma-Wave Opti-Probe). On each wafer, optical data were acquired on the same 49 locations before and after plasma processing. Subtraction was then performed for each location on the wafer, and an average value was computed over the 49 locations. At least three separate wafers were processed under each set of experimental conditions, and each etch-rate data point reported in this work corresponds to an average value over these wafers. The inherent uncertainty of the etch-rate data point is defined as the standard deviation across the three wafers divided by the average value.

X-ray photoelectron spectroscopy (XPS) was performed to obtain chemical information on poly-Si samples that had been plasma processed. Samples were analyzed in a Thermo-Scientific system that used monochromatic Al (8.3383 Å, 1486.7 eV) as the x-ray beam with an angle of incidence of 30° and beam size of $400 \times 600\ \mu m^2$. The binding energy (BE) scale was calibrated against Au $4f_7$ (BE = 83.9 eV), Ag $3d_5$ (BE = 386.7 eV), Cu $2p^3$ (BE = 932.7 eV), and C 1s (BE = 285.0 eV). The electron take-off-angle was 90° to the surface plane and the angle of electron collection was 60°. High-resolution chemical spectra were collected on the plasma-processed poly-Si samples to determine the chemical states of the various elements. The pass energy used was 50 V and the dwell time per step was 50 ms. To obtain chemical information as a function of depth (i.e., depth profile), the poly-Si sample was etched by an Ar^+ beam while performing *in situ* XPS. To minimize any ion-beam-induced degradation or preferential sputtering, the ion beam energy was set to 0.5 kV with an Ar^+ angle of incidence of 30°. For

each sample, the surface was etched with the Ar^+ beam until the poly-Si layer was etched through to reveal the underlying thermal oxide layer. By using a standard poly-Si film, the Ar^+ etch rate of the poly-Si film was determined to be ~0.75 Å/s. Using this method, the amount of time needed to completely etch the poly-Si layer using the Ar^+ beam is directly proportional to the thickness of the poly-Si that still remains post-plasma processing.

Definitions of variables used in this paper are as follows. The N_2 gas concentration is defined as volumetric flow rate of N_2 gas divided by the total volumetric flow rate of all gases. The photoresist ash rates reported in this work have accounted for the photoresist shrinkage; otherwise, the ash rates obtained would be overestimates of the actual values.[28] The shrinkage rate was measured under the same set of conditions as that employed for the dry-ash experiment (Figs. 1 and 2), except that the source power was turned off. We report the photoresist ash rate as a normalized value, expressed as the ratio of the actual etch rate to the etch rate, ER_o, which is a constant defined as the following. As described in Sec. V, we determined that the H_2/N_2 chemistry is a viable process for minimizing material loss, and a process window has been identified for this chemistry that achieves high ash rates and low poly-Si and Si_3N_4 etch rates. ER_o was measured at a set of conditions, $T = 300\,^{\circ}C$ and pressure = 1.5 Torr, that lies within this process window. In other words, the normalized ash rate is a relative measure of how the actual ash rate compares to the ash rate that gives rise to fast ashing and slow Si and Si_3N_4 etching.

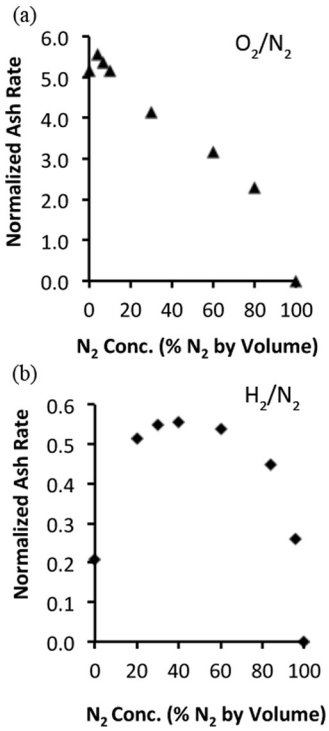

FIG. 1. DUV photoresist strip in downstream O_2- (a) and (b) H_2-based plasmas. Ash rate data were collected as a function of varying N_2 addition while fixing the temperature at 285 °C and keeping the total flow rate constant. The normalized ash rate is reported as a ratio of the actual ash rate to a constant ash rate, ER_o (see Sec. II). The inherent uncertainty of the ash rate data points ranges between 0.1% and 1.1% for the O_2-based plasma (a) and 0.4% and 4.8% for the H_2-based plasma (b).

III. RESULTS

A. DUV photoresist strip (dry ash)

Photoresist dry ash was performed in H_2- and O_2-based plasmas with varying concentrations of N_2 while fixing the temperature at 285 °C (Fig. 1). For the O_2-based chemistry, a slight addition of N_2 (~5%) leads to about 8% enhancement in ash rate when compared to that obtained with pure-O_2 plasma [Fig. 1(a)]. Further addition of N_2 beyond 5%, however, leads to a decrease in ash rate. As N_2 is added to H_2 plasma, the ash rate increases to reach a maximum at between 30% and 40% N_2, while further addition of N_2 leads to a decrease in ash rate [Fig. 1(b)]. The maximum ash rate that is attained at 30% N_2 corresponds to an enhancement of a factor of ~3 over that obtained with pure-H_2 plasma. It should be noted that the ash rate in pure-N_2 plasma is practically zero.

From Figs. 1 and 2, it can be seen that the O_2-based chemistry generally gives rise to higher ash rates than those obtained using the H_2-based chemistry, and the difference becomes more pronounced at higher temperatures. For example, the maximum ash rate that is obtained at $T = 285\,^{\circ}C$ with the O_2/N_2 plasma chemistry with 5% N_2 is ~38 000 Å/min, while that obtained using the H_2/N_2 chemistry with 30% N_2 is ~3800 Å/min. The generally higher ash rates exhibited by the O_2-based chemistry when compared to the H_2-based chemistry indicate that the O atoms are more efficient in ashing photoresist than the H atoms.

To extract the activation energy for photoresist strip, ash rate data were collected as a function of temperature for the O_2/N_2, H_2/N_2, and pure-H_2 plasma chemistries (Fig. 2). The N_2 concentrations were fixed at 5% and 30% for the O_2/N_2 and H_2/N_2 chemistries, respectively, and each corresponds to a concentration that yields the maximum ash rate for the respective chemistry. Regardless of the plasma chemistry, photoresist strip in downstream plasma is observed to be a thermally activated reaction, as evidenced by the continuous increase in ash rate as the temperature increases (Fig. 2). From the Arrhenius plot [Fig. 2(b)], the activation energy for the O_2/N_2 chemistry was extracted to be ~10 kcal/mol, which is much higher than that obtained for the H_2-based plasma chemistries. Specifically, the activation energy for the both the H_2/N_2 and the pure-H_2 chemistries was measured to be almost identical at ~5 kcal/mol.

Comparing the ash rates obtained under the H_2/N_2 (30% N_2) and pure-H_2 plasma chemistries, the ash rate exhibited by the former is higher at all temperatures tested (Fig. 2). For the same temperature, the ash rate obtained with the H_2/N_2 chemistry is about a factor of 3.5 higher than that attained by the pure-H_2 chemistry in the range of $100 \leq T \leq 330\,^{\circ}C$. For example, at 300 °C, the normalized ash rate for the H_2/N_2 chemistry is 1.00 while that for the pure-H_2 chemistry is 0.28 (Fig. 2). Although the H_2/N_2 chemistry yields ash rates that are generally lower than those attained using the O_2/N_2 chemistry, the H_2/N_2 chemistry with 30% N_2 can still achieve relatively fast ash rates that are in excess of 6700 Å/min at $T > 300\,^{\circ}C$.

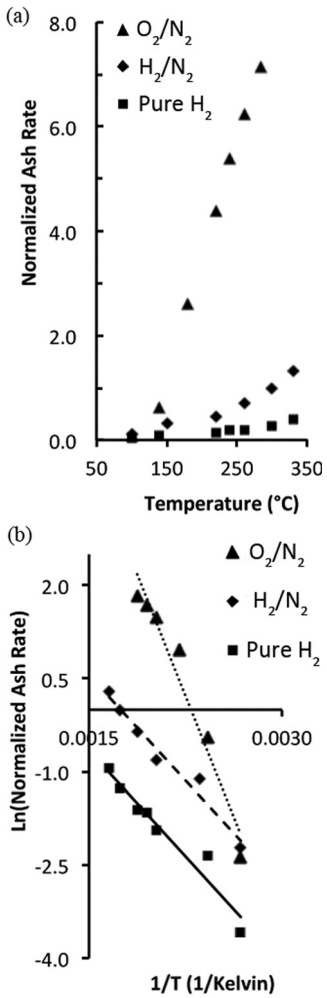

FIG. 2. (a) DUV photoresist ash rate measured as a function of temperature for the O_2/N_2, H_2/N_2, and pure-H_2 plasma chemistries. Arrhenius plots of the ash rate data are shown in (b). Concentrations of N_2 are 5% and 30% for the O_2/N_2 and H_2/N_2 plasma chemistries, respectively. The ash rate is reported as a ratio of the actual ash rate to a constant ash rate, ER_o (see Sec. II). The inherent uncertainty of the ash rate data points ranges between 0.2% and 10.0% for the O_2/N_2; 0.9% and 5.3% for H_2/N_2; and 1.1% and 4.6% for pure-H_2 chemistries.

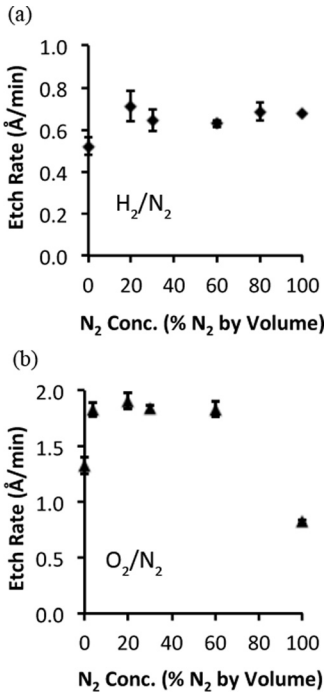

FIG. 3. Si_3N_4 etch in remote (a) H_2- and (b) O_2-based plasmas. Etch rate was measured as a function of varying N_2 concentration while fixing the temperature at $T = 300\,^{\circ}C$ and keeping the total flow rate constant. The error bar represents the standard deviation of the etch-rate measurements.

B. Silicon nitride removal

At a fixed temperature of 300 °C, the effect of varying N_2 concentration on the Si_3N_4 removal rate for the H_2/N_2 and O_2/N_2 plasma chemistries was investigated (Fig. 3). In general, the removal rate obtained using the H_2/N_2 plasma is considerably low, ~0.7 Å/min, and is relatively invariant with N_2 concentration. The slight variation in removal rate as a function of N_2 concentration that is observed in Fig. 3(a) may simply be attributed to measurement error, considering that the removal amounts corresponding to these data points are very low, ≤1.7 Å. For the O_2/N_2 plasma chemistry, the Si_3N_4 removal rate was measured to be higher, ~1.9 Å/min, and is relatively invariant with N_2 concentration in the range of 4–60% N_2 [Fig. 3(b)]. The removal rate decreases to ~1.3 Å/min in 100% O_2 plasma environment, and it is even lower in 100% N_2 plasma environment, ~0.8 Å/min. The lower Si_3N_4 removal rates that were measured with the H_2-based chemistry under the experimental conditions tested here highlight its ability to better suppress Si_3N_4 loss, as compared to the O_2-based chemistry.

The consumption of Si_3N_4 in pure-O_2 and O_2/N_2 plasmas could occur via two separate mechanisms. In pure-O_2 plasma, the top surface of the Si_3N_4 film is potentially oxidized and converted to a SiO_2-like layer. Specifically, N atoms are thought to be lost to the plasma due to the instability of the N atoms at the surface of the Si_3N_4 film, resulting in the consumption of the Si_3N_4. At the same time, O atoms replace the lost N atoms, which converts the top surface of the Si_3N_4 into a SiO_2-like layer.[29] In the O_2/N_2 plasma, however, Si_3N_4 could be physically removed from the surface as it gets converted into volatile etch products. NO and the energetic metastable NO* have been found to be generated in O_2/N_2 plasmas. These species can react directly with the N atoms from the Si_3N_4 surface and break Si–N bonds, resulting in the direct removal of Si_3N_4. During this process, volatile etch products, N_2O and/or N_2, are formed.[30–32] In addition to the physical removal of the Si_3N_4 by means of volatile product generation, Si_3N_4 could also be consumed through oxidation, much like that observed in the pure-O_2 plasma.

C. Poly-silicon removal

Si was previously found to be oxidized by pure-O_2 and O_2/N_2 plasmas,[33,34] and such oxidation consumes Si, which makes O_2-based plasmas unsuitable for many photoresist-strip applications in the advanced technology nodes. This oxidation issue, therefore, negates the need for us to characterize the interactions between poly-Si and the O_2-based

TABLE I. Comparison of poly-Si etch rates obtained using the pure-H2 plasma and H2 plasma with a small addition of N_2 (H_2/N_2).

	Pure-H_2 plasma		H_2/N_2 plasma		
Temperature (°C)	Etch rate (Å/min)	Standard deviation (Å/min)	Etch rate (Å/min)	Standard deviation (Å/min)	Pure-H_2:H_2/N_2 etch-rate ratio
60	44.4	5.54	2.0	0.08	22
150	35.7	0.82	2.4	0.03	15
300	21.4	0.66	2.6	0.04	8

plasma in this work. Knowing from the above that the H_2-based chemistry has a benefit of conserving material loss, we instead focused on investigating the effect of N_2 addition to H_2 plasma on the poly-Si removal behaviors (Table I).

For $T \geq 60\,°C$, the etch rate obtained with the pure-H_2 chemistry decreases from ~45 to 21 Å/min with increasing temperature. When a small amount of N_2 is added to the H_2 plasma, however, the poly-Si etch rate was dramatically suppressed to ~2 Å/min. For the H_2/N_2 chemistry, since the measured etch amounts are low, the slight variation in etch rate seen in Table I may simply be attributed to measurement error. As the temperature increases from 60 to 300 °C, the ratio of the etch rates obtained using the pure-H_2 to H_2/N_2 chemistries changes from 22 to 8. As a reference, at $T = 60\,°C$, the poly-Si etch rate in pure-N_2 plasma is negligible, ~0.8 Å/min.

XPS was used to provide insight into the change in the chemical composition of the poly-Si surface as a result of the plasma exposure and to verify the above finding that the H_2/N_2 plasma chemistry gives rise to much lower poly-Si etch rates when compared to the pure-H_2 chemistry. Poly-Si substrates that were exposed to pure-H_2, H_2/N_2, and pure-N_2 plasmas were subsequently analyzed by XPS depth profiling in which an Ar^+ beam was used to etch the surface while performing *in situ* XPS. Using this method, the Ar^+ etched the surface until the poly-Si layer was broken through to reveal the underlying thermal oxide layer [Fig. 4(a)]. In the topmost surface of the poly-Si substrate that was plasma processed, we observe a thin "mixed" layer comprising Si, O, C, and N, and this layer transitions to a pure poly-Si layer that extends all the way until the breakthrough point is reached. Chemical state information was derived from the high-resolution Si 2p spectra of the samples. For each sample, the Si 2p spectrum reveals a broad peak at BE ~ 104 eV and another peak at BE ~ 99.6 eV, which corresponds to the Si(0) substrate [Fig. 4(b)]. The former peak can be decomposed into three major components: ~101.8, 103.0, and 104.0 eV. The first peak at BE ~ 101.8 eV corresponds to either Si_3N_4 (Ref. 35) or silicon suboxide (e.g., Si^{3+}),[36] while the second peak at BE ~ 103.0 eV could correspond to SiO_2 (Ref. 36) or silicon oxynitride.[37] Chang *et al.* observed a peak at BE ~ 104.0 eV and attributed it to the Si–O bond detected in silicon oxynitride film grown from silicon oxide.[38] Without further investigation, we cannot be more definitive than to state that the top mixed layer of the poly-Si surface potentially comprises a mixture of SiO_2, Si_3N_4, and/or silicon oxynitride.[39]

The relatively high concentration of O detected in the poly-Si surface is quite surprising [Fig. 4(a)], considering that O_2 gas was not flowed into the chamber at any time during plasma processing. Presumably, the oxygen found in the surface could have originated from oxygen liberated from the quartz dome or the ambient air that was introduced into the reactor due to the inherent leak of the chamber, which was measured to be <20 mTorr/min.

From the depth profile obtained using the Ar^+ beam, we can determine the thickness of the remaining poly-Si film post-plasma process. From Fig. 4(c), the times that are needed to Ar^+ etch the poly-Si layers that remained post-plasma process are 1964, 1893, and 1679 s, for the substrates processed with pure-N_2, H_2/N_2, and pure-H_2 plasmas, respectively. This finding indicates that the thickness of the poly-Si film, that remained post-plasma process, decreases in thickness in that order. Since the original (preplasma process) thickness of the poly-Si layer is roughly the same across these wafers, ~1485 ± 0.5 Å, we deduced that the pure-H_2 plasma led to the highest Si loss, followed by the H_2/N_2 plasma, and then the pure-N_2 plasma. Thus, we have verified the finding in Table I that when compared to the pure-H_2 plasma, the H_2/N_2 plasma has the capability to significantly suppress Si loss.

IV. DISCUSSION

A. Photoresist strip using O_2/N_2, H_2/N_2, and pure H_2 plasmas

1. Reaction mechanisms

In our ICP reactor where the wafer is exposed to a remote/downstream plasma condition, the surface interacts with mostly neutral plasma species and etching occurs purely by chemical reactions.

Etching of photoresist in downstream pure-O_2 plasma occurs by a mechanism that has been well studied elsewhere.[40–42] Briefly, the initial reaction involves a hydrogen-abstraction step at a hydrocarbon-containing site, resulting in the formation of an alkyl radical. Oxygen addition to the radical sites oxidizes the polymer molecule to generate peroxide and alkoxy radicals. The peroxide radicals undergo various propagation pathways that covert the peroxide into additional alkoxy radicals as well as generate more alkyl radicals (i.e., oxidation chain reaction). The formation of alkoxy radicals then causes the cleavage of the polymer chain to generate volatile fragments, which ultimately removes the photoresist. Much work has been done

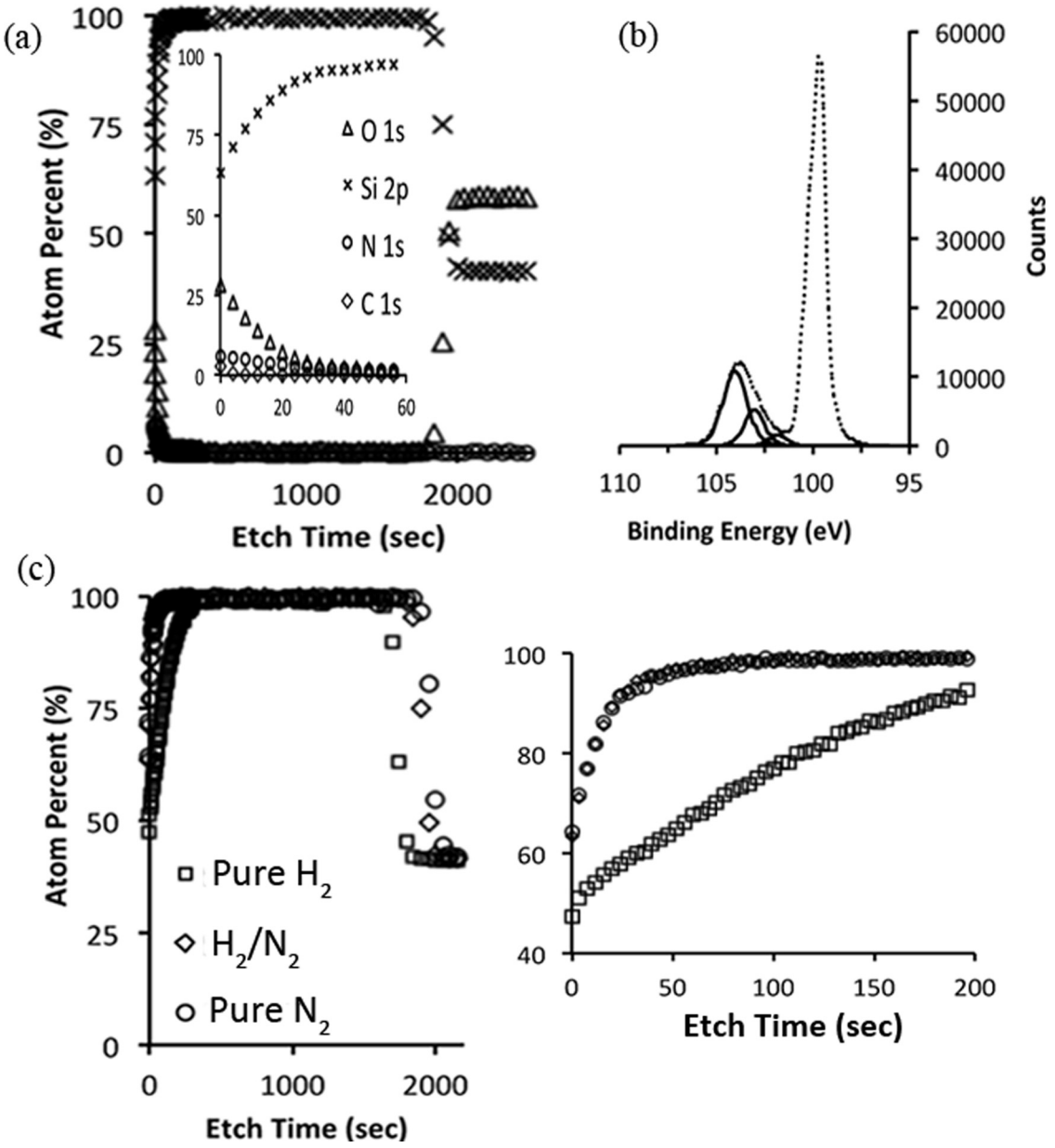

FIG. 4. XPS analyses of poly-Si films that were exposed to pure-H_2, H_2/N_2, and pure-N_2 plasmas at 60 °C. Other process parameters (e.g., pressure and total flow rate) were kept constant for all samples. (a) A representative depth profile for poly-Si film that was processed with the H_2/N_2 plasma. Poly-Si breakthrough occurs when the Si 2p signal decreases abruptly and the O 1s signal increases at ~2000 s. The inset depicts the magnified depth profile at short Ar^+ etch times. (b) A Si 2p spectrum (dashed line) obtained from the high-resolution scan of the poly-Si processed with H_2/N_2 plasma prior to subjecting it to the Ar^+ etch. Deconvolved peaks are depicted as solid lines. (c) Depth profiles of poly-Si films that were processed with various plasma conditions obtained by XPS depth profiling; only the Si 2p signals are shown here. The inset depicts the magnified depth profiles at short Ar^+ etch times. From the inset (right), the Si depth profiles for the H_2/N_2 and pure-N_2 plasmas practically overlapped each other, i.e., they are nearly identical.

to determine that oxygen atoms, as opposed to molecular oxygen, are the main etchant species for the photoresist strip in pure-O_2 plasma.[40,41,43]

For the O_2-based chemistry, the photoresist ash rate reaches a maximum with the addition of roughly 5% N_2 [Fig. 1(a)], and this is attributed to the increase in the density of O atoms, [O]. An addition of N_2 that is $\leq$10% was found to increase the [O] relative to that in pure-O_2 plasma. In addition, the behavior of the photoresist ash rate as a function of N_2 fraction was determined to correlate directly with the behavior of [O] as a function of N_2 fraction.[44,45] These findings suggest that the O atoms are still the main etchant species for photoresist strip in O_2/N_2 plasma and that the increase in ash rate induced by a small N_2 addition is due to the increase in [O]. Furthermore, Fujimura *et al*. found that the addition of N_2 to O_2 plasma had no effect on the activation energy for the photoresist strip, which affirms that N_2 addition does not change the dry-ash mechanism.[44,46]

As described in our previous publication,[17] chemical etching of photoresist in downstream pure-H_2 plasma occurs by successive reaction steps that initially involve the attack of atomic hydrogen at hydrocarbon-containing sites on the polymer backbone.[25,47] In the first step, a hydrogen-abstraction reaction occurs at an available hydrocarbon-containing site to

generate an alkyl radical. This step is followed by the addition of atomic hydrogen to the alkyl radical, which is exothermic and generates ~100 kcal/mol of energy. Dissipation of this energy is then believed to result in the scission of C–C bonds (~80 kcal/mol)[6] found in the polymer backbone. As a result, polymer fragmentation and volatilization occur.

The process trend of photoresist ash rate as a function of N_2 concentration can give insight to the mechanism for the photoresist strip when N_2 is added to the H_2 plasma (i.e., H_2/N_2 plasma). From Fig. 1, the ash rate corresponding to the pure-N_2 plasma is zero, suggesting that N atoms alone cannot etch the photoresist in a remote-plasma environment. It was shown that as the N_2 addition to the H_2 plasma increases from 0 to ~30%, the H radical density, [H], increases to a maximum. Further addition of N_2, however, causes [H] to decrease.[18,19,28] Similarly, the photoresist ash rate also increases with increasing N_2 addition until a maximum is reached at between 30% and 40% N_2, and further addition of N_2 leads to a decrease in ash rate [Fig. 1(b)]. The direct correlation between the behaviors of [H] and the photoresist ash rate as a function of the N_2 concentration suggests that the H atoms are the dominant etchant species. In addition, it is unlikely for the N atoms present in the H_2/N_2 plasma to etch the photoresist to any significant degree. This is because the N radical density was found to increase continuously with increasing N_2 addition,[18,19] and this behavior is inconsistent with the trend for the photoresist ash rate as a function of N_2 concentration [Fig. 1(b)]. The above findings collectively indicate that it is the H atoms that are the main etchant species, and that the increase in ash rate with 30–40% N_2 addition is attributed to the increase in [H].

The increase in [H] with N_2 addition up to ~30% that is followed by the drop in [H] with further addition of N_2 is a result of the interplay between the change in H_2 dissociation ratio and the molecular density of H_2 as function of N_2 concentration. Nagai *et al.* found that the total electron density in the plasma environment increased substantially when a small amount of N_2 was added to H_2 plasma.[18] They attributed this increase to the larger ionization cross section of N_2 when compared to H_2 molecules. The high electron density in turn enhances the dissociation of the H_2 into H atoms. Alternatively, Kuo *et al.* suggest that the N_2 molecules are excited to metastable states by electron impacts, and the quenching of these metastable states provides additional pathways that increase the H_2 dissociation ratio.[19] Regardless of the exact mechanism, the addition of a small amount of N_2 results in the enhanced dissociation of H_2 and, ultimately, gives rise to an increase in [H], which in turn increases the photoresist ash rate. However, as more N_2 is added (>30%), although the electron density remains high,[18] the concentration of H_2 molecules in the reactor must decrease in order to keep the total chamber pressure constant (i.e., dilution of H_2). Hence, the net [H] drops as the N_2 concentration increases beyond about 30–40%.

2. Activation energy for photoresist strip

For all the downstream plasma chemistries studied here, the photoresist-strip reaction is seen to be a thermally activated process that exhibits a continuous increase in ash rate as a function of temperature. This behavior is a characteristic of downstream plasma ashing where photoresist is removed by chemical reactions only, and it has been observed for many plasma systems, e.g., pure O_2,[21,40] O_2/H_2O,[46] O_2/H_2,[46] O_2/N_2,[44] O_2/CF_4,[48,49] pure H_2,[6,17] H_2/N_2,[19] etc.

As described in Sec. III A, the activation energy (E_a) for the O_2/N_2 photoresist strip was measured to be ~10 kcal/mol. Spencer *et al.* reported an E_a of ~11.6 kcal/mol for photoresist strip in downstream pure-O_2 plasma, but noted that there are significant discrepancies on the reported E_a values: between 6.5 and 11.6 kcal/mol.[21,50] A reason could be the level of loading effect in the reactor, and the loading effect refers to a condition in which the rate of the heterogeneous photoresist-strip reaction occurs faster than the rate at which gas reactants can be transported to the wafer surface. Fujimura *et al.* also reported 11.5 kcal/mol as the E_a value for both downstream O_2 and O_2/N_2 chemistries, and they found that the effect of N_2 addition to the O_2 plasma is only to increase [O] and that it does not alter the activation energy.[44,46] Koretsky *et al.* reported a lower E_a value of 10.6 kcal/mol, which is close to the value determined in this work.[48] Considering that the E_a values could differ depending upon the specific experimental conditions, the E_a value of 10 kcal/mol found here can be considered to be consistent with the values reported in the literature.

Both the H_2/N_2 and pure-H_2 chemistries exhibit identical activation energy of ~5 kcal/mol, which is a factor of 2 lower than that for the O_2/N_2 chemistry. The lower E_a for the H_2-based process indicates that the increase in ash rate as a function of temperature is slower for this process than for the O_2-based process (Fig. 2). The fact that both the H_2/N_2 and the pure-H_2 chemistries exhibit the same activation energy implies that the mechanism for photoresist strip for these two chemistries is likely to be identical. This claim also substantiates our finding in the above; that, like in the case of pure-H_2 plasma, the main etchant species for photoresist removal in the H_2/N_2 plasma are also the H atoms.

B. Si removal in pure-H_2 and H_2/N_2 plasmas

Previously, we found that the Si etch rate in pure-H_2 plasma decreases continuously with increasing temperature in the region of $60 \leq T \leq 300\,^{\circ}C$, and this behavior is consistent with that seen in Table I.[17] The mechanism of Si etch in pure-H_2 plasma has been discussed in our previous work.[17] Briefly, Si etching occurs by means of the successive addition of hydrogen atoms to Si forming Si-H_x complexes, where the number of chemisorbed hydrogen atoms (x) grows from $x = 1$ to 3, i.e., SiH, SiH_2, and SiH_3. The addition of an H atom to SiH_3 then generates volatile silane, SiH_4, which leads to the etching of Si.[51–53] The decreasing etch rate as a function of temperature is caused by the increasing heterogeneous recombination of H atoms on the Si surface that release H_2 (g), and this recombination consumes the chemisorbed H atoms needed for the formation of volatile SiH_4.[51–56] As a result, the Si etch rate decreases with increasing temperature in the region of $T > 60\,^{\circ}C$.

We showed unambiguously by both ellipsometry and XPS that a small addition of N_2 to the H_2 plasma suppressed the Si etch rate dramatically (Table I and Fig. 4). Due to the complexity of the interactions that occur among the various plasma-activated species and the Si surface, the mechanism for the reduction in Si loss in H_2/N_2 plasma is still elusive. At a low temperature of 60 °C, where the poly-Si etch rate in pure-H_2 plasma is very high (~45 Å/min), pure-N_2 plasma was found to practically not etch poly-Si, suggesting that the N atoms alone do not etch poly-Si. As described in Sec. IV A, [H] is increased when a small amount of N_2 ($\leq$30%) is added to the hydrogen plasma. If Si etch rate were only governed by the [H] and there were no other underlying interactions, then the higher [H] in the H_2/N_2 plasma, as compared to that in pure-H_2 plasma, would lead to a higher etch rate. However, the fact that we observe a lower Si loss with the H_2/N_2 plasma than with the pure-H_2 plasma suggests that there are other interactions in play that account for the lower Si loss observed with the H_2/N_2 plasma.

A few phenomena/interactions that may account for the lower Si loss in the H_2/N_2 plasma include the following. It is possible that the H_xN_y species[5,57] present in the H_2/N_2 plasma could react with the poly-Si surface and occupy the binding sites that would be available for the H atoms to adsorb on the Si surface. Since Si etching by H atoms requires the chemisorption of H atoms on the Si surface, the Si etch rate would then be suppressed. We should also take into account the complex interactions among the N atoms, H atoms, H_xN_y species, and the Si surface, which could ultimately affect the Si etch rate. For example, although we found that the N atoms by themselves do not etch Si (at least, at low temperatures), N atoms have been shown to interact with silicon in various ways, such as forming Si-N complexes,[58,59] passivating Si defects,[60] and diffusing rapidly in bulk Si.[61] These phenomena could in turn affect the ways the H atoms interact with the Si surface in a complex manner. Furthermore, XPS analyses showed that the top surface of the poly-Si post-plasma process potentially contains a mixture of SiO_2, Si_3N_4, and/or silicon oxynitride (Fig. 4). The presence of this mixed surface layer could presumably impact the ways the active plasma species interact with the Si surface. Clearly, due to the complexity of the interactions between the plasma species and Si surface, a much more in-depth investigation is needed to pinpoint the exact mechanism on how N_2 addition to the H_2 plasma suppresses Si loss. We reserve this investigation for our future work.

V. SUMMARY AND CONCLUSIONS

FEOL photoresist-strip applications (e.g., HDIS and LDD implant strip) for the 45 nm technology node and beyond require that the photoresist removal rate is maximized, the loss of materials such as Si and Si_3N_4 is minimized, and the plasma chemistry is compatible with semiconductor substrates and HKMG materials. In this work, we evaluated and compared the etch behaviors of photoresist, poly-Si, and Si_3N_4 in downstream O_2/N_2, H_2/N_2, and pure-H_2 plasmas. From the data, we have determined which chemistry is more appropriate for meeting the above requirements as well as the process conditions for that chemistry to maximize the photoresist ash rate and suppress material loss.

The photoresist ash rate behaviors as a function of temperature and N_2 addition were elucidated for both the H_2- and O_2-based chemistries. A small addition of N_2 increases the hydrogen and oxygen radical densities in the H_2/N_2 and O_2/N_2 plasmas, respectively, thus augmenting the photoresist ash rate. Specifically, the maximum ash rate is attained at ~30–40% N_2 addition for the H_2-based plasma and 5% N_2 addition for the O_2-based plasma. Regardless of the plasma chemistry, downstream photoresist strip is a thermally activated reaction, which is evidenced by the continuous increase in ash rate with increasing temperature. The photoresist strip using the O_2/N_2 chemistry yields an activation energy of ~10 kcal/mol, which is a factor of 2 higher than the ~5 kcal/mol obtained for both the H_2/N_2 and the pure-H_2 chemistries. Under the experimental conditions employed here, the O_2-based plasma generally exhibits ash rates that are higher than those obtained in the H_2-based plasma.

When compared to the O_2-based plasma, the H_2-based plasma was shown to be more effective in conserving material loss. In the experimental conditions that we tested, the H_2-based plasma gives rise to much lower Si_3N_4 etch rates than the O_2-based chemistry. Specifically, the H_2-based chemistry yields a low Si_3N_4 etch rate of ~0.7 Å/min, even at a high temperature of 300 °C. Knowing that the H_2-based chemistry has the benefit of suppressing Si_3N_4 loss, we proceeded to investigate the effect of N_2 addition to the hydrogen plasma on the poly-Si etch rate. It was found that a small N_2 addition to the H_2 plasma suppresses the poly-Si etch rate significantly, as shown unambiguously by both the ellipsometry and the XPS data. Due to the complex interactions that could occur between the various plasma-activated species (e.g., N atoms, H atoms, H_xN_y species) and the Si surface, the exact mechanism for the reduction in Si loss that is seen with the H_2/N_2 plasma is still elusive at the moment. Nonetheless, we have demonstrated that the H_2/N_2 plasma chemistry is more desirable than the pure-H_2 counterpart due to the ability of the former to generate higher ash rates and suppress Si loss.

For the advanced technology nodes, minimal material loss and chemical compatibility with the various device layers are fast becoming crucial requirements that must be met by the FEOL fabrication processes. As shown in this paper, when compared to the O_2/N_2 chemistry, the H_2/N_2 chemistry has a benefit of conserving material (e.g., Si_3N_4) loss. In addition, O_2-based plasmas cause the oxidation of semiconductor substrates[33,34] and HKMG materials,[4,11] attributes that are unacceptable for FEOL processing in the advanced nodes. We believe that these advantages of the H_2-based plasma justify the trade off for its lower ash rates than the ash rates obtained by the O_2-based plasma.

From the etch-rate data obtained in this work, we can determine the appropriate process conditions for the H_2/N_2 chemistry to maximize ash rate and minimize material loss. Since downstream photoresist strip is a thermally activated

reaction, the H_2/N_2 dry ash should be performed at high temperatures ($T \geq 300\,^{\circ}C$) to maximize the ash rate. The material etch rates exhibited by the H_2/N_2 chemistry are still considerably low at high temperatures; specifically, at $T = 300\,^{\circ}C$, the Si_3N_4 and Si etch rates are ~0.7 and 2 Å/min, respectively. These findings suggest that the high-temperature regime corresponds to the desirable process window for maximizing ash rate and still maintaining low material loss. For devices that contain HKMG structures, this process window may need to be optimized further in order to ensure that the chemical integrity of the structure is maintained. We believe that the H_2/N_2 plasma chemistry has a wide process window that allows it to be useful for various photoresist-strip applications in the advanced nodes. From our previous work on pure-H_2 plasma, various process parameters have dramatic effects on the etch rates of photoresist, Si, and Si_3N_4.[17] Similarly, their etch rates in the H_2/N_2 plasma are also expected to be highly influenced by parameters such as temperature, pressure, and N_2 concentration. By tuning these parameters judiciously, we believe that the H_2/N_2 plasma is a viable chemistry that has the potential to meet the stringent requirements for FEOL photoresist-strip applications in the advanced technology nodes.

ACKNOWLEDGMENTS

The authors are immensely grateful to Ed Bacani and Phuong Luu who assisted us with the operations of the reactor and wafer measurements. They thank Charles Brundle for his guidance and advice on the interpretation of the XPS data. Finally, they thank Joon Park for providing much support for this project that allowed it to proceed quickly.

[1] *International Technology Roadmap for Semiconductors: Interconnect* (Semiconductor Industry Association, 2005).
[2] S. Guha and V. Narayanan, Annu. Rev. Mater. Res. **39**, 181 (2009).
[3] G. D. Wilk, R. M. Wallace, and J. M. Anthony, J. Appl. Phys. **89**, 5243 (2001).
[4] B. H. Lee, S. C. Song, R. Choi, and P. Kirsch, IEEE Trans. Electron Devices **55**, 8 (2008).
[5] N. Posseme, T. Chevolleau, T. David, M. Darnon, O. Louveau, and O. Joubert, J. Vac. Sci. Technol. B **25**, 1928 (2007).
[6] X. Hua *et al.*, J. Vac. Sci. Technol. B **24**, 1238 (2006).
[7] M. A. Worsley, S. F. Bent, S. M. Gates, N. C. M. Fuller, W. Volksen, M. Steen, and T. Dalton, J. Vac. Sci. Technol. B **23**, 395 (2005).
[8] P.-T. Liu, T. C. Chang, Y. S. Mor, C. W. Chen, T. M. Tsai, C. J. Chu, F. M. Pan, and S. M. Sze, Electrochem. Solid-State Lett. **5**, G11 (2002).
[9] D. Shamiryan, M. R. Baklanov, S. Vanhaelemeersch, and K. Maex, J. Vac. Sci. Technol. B **20**, 1923 (2002).
[10] S. Xu and L. Diao, J. Vac. Sci. Technol. A **26**, 360 (2008).
[11] J. Hackenberg and J. Linn, J. Vac. Sci. Technol. A **6**, 1388 (1988).
[12] O. Louveau, C. Bourlot, A. Marfoure, I. Kalinovski, J. Su, G. Hills, and D. Louis, Microelectron. Eng.**73–74**, 351 (2004).
[13] P. Lazzeri, G. J. Stueber, G. S. Oehrlein, R. McGowan, E. Busch, S. Pederzoli, M. Bersani, and M. Anderle, J. Vac. Sci. Technol. B **24**, 2695 (2006).
[14] B. K. Kirkpatrick, J. J. Chambers, S. L. Prins, D. J. Riley, W. Xiong, and X. Wang, Solid State Phenom. **145–146**, 245 (2009).
[15] *International Technology Roadmap for Semiconductors: Front End Processes* (Semiconductor Industry Association, 2005).
[16] *International Technology Roadmap for Semiconductors: Front End Processes* (Semiconductor Industry Association, 2011).
[17] B. A. Thedjoisworo, D. Cheung, and D. Zamani, J. Vac. Sci. Technol. A **30**, 031303 (2012).
[18] H. Nagai, S. Takashima, M. Hiramatsu, M. Hori, and T. Goto, J. Appl. Phys. **91**, 2615 (2002).
[19] M. Kuo, X. Hua, G. S. Oehrlein, A. Ali, P. Jiang, P. Lazzeri, and M. Anderle, J. Vac. Sci. Technol. B **28**, 284 (2010).
[20] J. W. Coburn and H. F. Winters, J. Vac. Sci. Technol. **16**, 391 (1979).
[21] J. E. Spencer, R. A. Borel, and A. Hoff, J. Electrochem. Soc. **133**, 1922 (1986).
[22] C. Cardinaud, M.-C. Peignon, and P.-Y. Tessier, Appl. Surf. Sci. **164**, 72 (2000).
[23] D. B. Graves, IEEE Trans. Plasma Sci. **22**, 31 (1994).
[24] P. F. Williams, *Plasma Processing of Semiconductors* (Springer, New York, 1997), p. 477.
[25] G. J. Stueber, G. S. Oehrlein, P. Lazzeri, M. Bersani, M. Anderle, E. Busch, and R. McGowan, J. Vac. Sci. Technol. B **25**, 1593 (2007).
[26] S. Xu *et al.*, J. Vac. Sci. Technol. B **25**, 156 (2007).
[27] L. Zheng, L. Ling, X. Hua, G. S. Oehrlein, and E. A. Hudson, J. Vac. Sci. Technol. A **23**, 634 (2005).
[28] J. Cho, J. Yang, H. Park, and S.-G. Park, Surf. Coat. Technol. **205**, 1532 (2010).
[29] G. P. Kennedy, O. Buiu, and S. Taylor, J. Appl. Phys. **85**, 3319 (1999).
[30] B. E. E. Kastenmeier, P. J. Matsuo, J. J. Beulens, and G. S. Oehrlein, J. Vac. Sci. Technol. A **14**, 2802 (1996).
[31] C. Reyes-Betanzo, S. A. Moshkalyov, J. W. Swart, and A. C. S. Ramos, J. Vac. Sci. Technol. A **21**, 461 (2003).
[32] B. E. E. Kastenmeier, P. J. Matsuo, G. S. Oehrlein, R. E. Ellefson, and L. C. Frees, J. Vac. Sci. Technol. A **19**, 25 (2001).
[33] D. W. Hess, IBM J. Res. Dev. **43**, 127 (1999).
[34] J. R. Ligenza, J. Appl. Phys. **36**, 2703 (1965).
[35] T. N. Wittberg, J. R. Hoenigman, W. E. Moddeman, C. R. Cothern, and M. R. Gulett, J. Vac. Sci. Technol. **15**, 348 (1978).
[36] K. Ohishi and T. Hattori, Jpn. J. Appl. Phys., Part 2 **33**, L675 (1994).
[37] T. Hattori, H. Nohira, S. Shinagawa, M. Hori, M. Kase, and T. Maruizumi, Microelectron. Reliab. **47**, 20 (2007).
[38] J. P. Chang *et al.*, J. Appl. Phys. **87**, 4449 (2000).
[39] C. R. Brundle, G. Conti, and P. Mack, J. Electron Spectrosc. Relat. Phenom. **178–179**, 433 (2010).
[40] M. A. Hartney, D. W. Hess, and D. S. Soane, J. Vac. Sci. Technol. B **7**, 1 (1989).
[41] S. J. Moss, A. M. Jolly, and B. J. Tighe, Plasma Chem. Plasma Process. **6**, 401 (1986).
[42] S. V. Babu and L. A. Tiemann, *Proceedings of the 7th International Symposium on Plasma Chemistry (ISPC)*, Eindhoven, The Netherlands, 1–5 July 1985, edited by C. J. Timmermans (International Union of Pure and Applied Chemistry (IUPAC), 1985), p. 1025.
[43] J. M. Cook and B. W. Benson, J. Electrochem. Soc. **130**, 2459 (1983).
[44] S. Fujimura, K. Shinagawa, M. Nakamura, and H. Yano, Jpn. J. Appl. Phys., Part 1 **29**, 2165 (1990).
[45] R. L. Brown, J. Phys. Chem. **71**, 2492 (1967).
[46] S. Fujimura, K. Shinagawa, M. T. Suzuki, and M. Nakamura, J. Vac. Sci. Technol. B **9**, 357 (1991).
[47] G. J. Kluth, M. M. Sung, and R. Maboudian, Langmuir **13**, 6491 (1997).
[48] M. D. Koretsky and J. A. Reimer, J. Appl. Phys. **72**, 5081 (1992).
[49] N. H. Lu, C. Nilsen, J. A. Welsh, S. V. Babu, and J. F. Rembetski, *Proceedings of the Fifth Symposium on Plasma Processing*, edited by G. S. Mathad, G. C. Schwartz, and G. Smolinsky (The Electrochemical Society, Inc., Pennington, NJ, 1985), Vol. 85-1, p. 175.
[50] T. H. Lin, M. Belser, and Y. Tzeng, IEEE Trans. Plasma Sci. **16**, 631 (1988).
[51] S. Veprek, C. Wang, and M. G. J. Veprek-Heijman, J. Vac. Sci. Technol. A **26**, 313 (2008).
[52] J. Abrefah and D. R. Olander, Surf. Sci. **209**, 291 (1989).
[53] S. M. Gates, R. R. Kunz, and C. M. Greenlief, Surf. Sci. **207**, 364 (1989).
[54] A. P. Webb and S. Vepřek, Chem. Phys. Lett. **62**, 173 (1979).
[55] S. Vepřek and F. A. Sarott, Plasma Chem. Plasma Process. **2**, 233 (1982).
[56] S. M. Gates, C. M. Greenlief, and D. B. Beach, J. Chem. Phys. **93**, 7493 (1990).
[57] H. Yamamoto *et al.*, J. Appl. Phys. **110**, 123301 (2011).
[58] H. M. Jennings, J. Mater. Sci. **18**, 951 (1983).
[59] H.-C. Cheng, F.-S. Wang, and C.-Y. Huang, IEEE Trans. Electron Devices **44**, 64 (1997).
[60] M.-J. Tsai, F.-S. Wang, K.-L. Cheng, S.-Y. Wang, M.-S. Feng, and H.-C. Cheng, Solid-State Electron. **38**, 1233 (1995).
[61] P. A. Schultz and J. S. Nelson, Appl. Phys. Lett. **78**, 736 (2001).